OPEN ACCESS
Saudi Journal of Engineering and Technology
Abbreviated Key Title: Saudi J Eng Technol
ISSN 2415-6272 (Print) |ISSN 2415-6264 (Online)
Scholars Middle East Publishers, Dubai, United Arab Emirates
Journal homepage: https://saudijournals.com

Original Research Article

Simulation and Measurement of *on-body* and *off-body* Communication Propagation Channels by using *dual-band* Magnetic Antenna Textile

Gita Ayu Ardiani[1*], Sandra Octaviani B W[1], Isdaryanto Iskandar[1]

[1]Faculty of Engineering, Atma Jaya Catholic University of Indonesia, Jakarta, Indonesia

DOI: 10.36348/sjet.2022.v07i07.003 | **Received:** 02.07.2022 | **Accepted:** 08.08.2022 | **Published:** 16.08.2022

***Corresponding author:** Gita Ayu Ardiani
Faculty of Engineering, Atma Jaya Catholic University of Indonesia, Jakarta, Indonesia

Abstract

Evolution of Wireless Body Area Network (WBAN) in telemedicine field keep increased along with needs and enhancement of services, nevertheless an efficient and effective form of communication becomes essential for any type of wireless communication network. One of the most important parameter for designing communication network is path loss exponent. Based on that, the purpose of this research is to know the propagation characteristics for on-body and off-body communication by comparing the simulation and measurement using magnetic textile antenna at 2.45 GHz and 924 MHz with distance variation in LOS and NLOS conditions. In this research, friis formula is used to get the path loss exponent value that shows the characteristics of propagation. The calculation of path loss exponent value for simulation and measurement for on-body communication with LOS and NLOS conditions are between 1.7-1.9 while off-body with LOS and NLOS conditions are between 2.1-5.2. These results show that the body affects path loss exponents value and have own characteristics.

Keywords: Textile Antenna, Path Loss Measurement, On-body Off-body Communication, Dual-Band.

I. INTRODUCTION

Information and communication technology (ICT) has great potential to overcome some problems faced by developed and developing countries such as providing access, cost effectiveness, and high-quality healthcare services [1]. There are several types of services that using the advancement of ICT, one of the examples is long distance communication-based heatlh services called telemedicine. Wireless Area Body Network (WBAN) is an example of development for telemedicine communication.

WBAN is a communication that puts the antenna on the area around or near the human body, and it has 3 kinds of schemes, namely on-body, in-body, and off-body.

WBAN communication system performance is influenced by the interaction of electromagnetic waves with the body. Therefore, it is important to know the effect of the body on the performance of the antenna, because every part of the body has different electrical characteristics. Thus, the modeling of body characteristics is necessary to obtain accurate results of antenna performance [3].

To achieve the proper planning of wireless communication network, including WBAN, it requires information of accurate path loss value from specific propagation environment. The accuracy is determined by an important parameter called path loss exponent.Path loss exponent has a strong effect to determine quality of network communication; therefore an accurate estimation is required for design and operation to achieve an efficient wireless communication [7].

One phenomenon from BAN communication propagation, called Human Body Shadowing, it happens when the human body affects communications from wireless devices, because the body can covering or blocking dominant signal path of the sending and receiving antenna[8]. So in this study, simulation will be done for on-body and off-body communication propagation channels by using magnetic textile antennas with LOS and NLOS conditions where propagation hampered the human body.

II. BASIC THEORY

A. Body Centric Wireless Communication (WBAN)

Body Centric Wireless Communicationis a wireless communication network that located around the body, either communication between devices is on surface of the body, in body, or body-to-body. The sensors can be used by attached it to body or implanted into the human body [5].

There are 3 topologies of body centric wireless communication, namely on-body communication, off-body communication and in-body communication.

1. On-body Communication is radio communication from wearable devices like antenna to another antenna that placed around surface of the human body [6].
2. Off-body Communication is communication between devices that placed around surface of human body and placed off of the body or another system with specific distance [6].
3. In-Body Communication is communication between device that implanted inside the body with another device or system outside the body [6].

Research on Body Centric Communication can be done using several frequency bands that are usually different for each country. In Indonesia, the frequency 2.45 GHz ISM band and the 924 MHz RFID band is an unlicensed band and indeed available for research advice so it is free to use the band to conduct research and development of wearable antennas [3].

B. Wearable Antenna

The important parameter to obtain maximum results for wearable antennas is size, matching, and antenna efficiency. In wearable antenna applications, flexible antenna shapes can be fabricated using materials from textiles because textile antennas can be easily integrated into clothing.

Human body model nastran is used in the form of adult male body, obtained from https://www.nevaelectromagnetics.com. Then the body model is simulated with CST Microwave Studio software. Phantom model shaped human body consisting of 3 layers of outermost tissue, this layer is the skin, fat, and muscle which is the part that most affect the performance of the antenna. The human body does not always raise the working frequency of an antenna. This depends on the type of antenna (electric or magnetic) and the distance of the antenna with the body [6].

C. Path Loss

To model the *path loss* between Tx and Rx into distance function, semi-empirical formula in dB is used, by according to *Friis formula* in *free space* [7]. i.e.:

$$P_{dB}(d) = P_{0,dB} + (10n)log_{10}(\frac{d}{d_0}) \quad (1)$$

$$P_{dB}(d) = -|S_{21}|_{dB} \quad (2)$$

In this model, $P_{0,dB}$ is *path loss* that is measured at reference distance, *n* is *path loss* exponent, *d* is the distance between *transmitting* and *receiving* antennas, and d_0 is reference distance [4]. Path loss value is equal to $-|S_{21}|_{dB}$.

Path loss exponent value is changed based on the characteristic of environment; this changing path loss shows how the attenuation equation from a communication.

Table I: The Characteristic of Path Loss Exponent in Some Environments [8]

Environments	*n*
Free-space	2
Urban area cellular radio	2.7-3.5
Shadowed urban cellular radio	3-5
In-building LOS	1.6-1.8
Obstructed in building	4-6
Obstructed in factories	2-3

III. METHODOLOGY

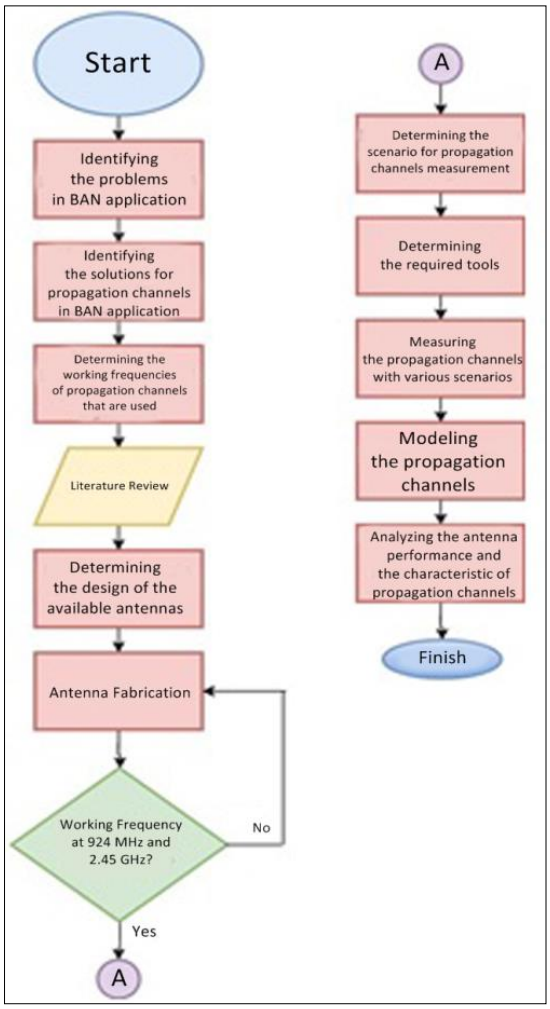

Figure 1: Flow Diagram

The antenna used for simulation of on-body and off-body communication design in this thesis was taken from the design owned by Abdurrahman Wahid [9] working in *dual-band* for RFID and ISM i.e., 924 MHz and 2.45 GHz. The antenna that had been made used a design as shown in Figure 2a. The right spiral had great impact towards 924 MHz, while the left spiral had great impact towards the performance of resonance frequency of 2.45 GHz.

The antenna was fabricated by using thread that was embroidered as the materials by according to the design pattern, and then it was cut and layered by using conductive material in form of silver paint. The fabrication result is shown in Figure 2b. The antenna worked at 924 MHz and 2.45 GHz.

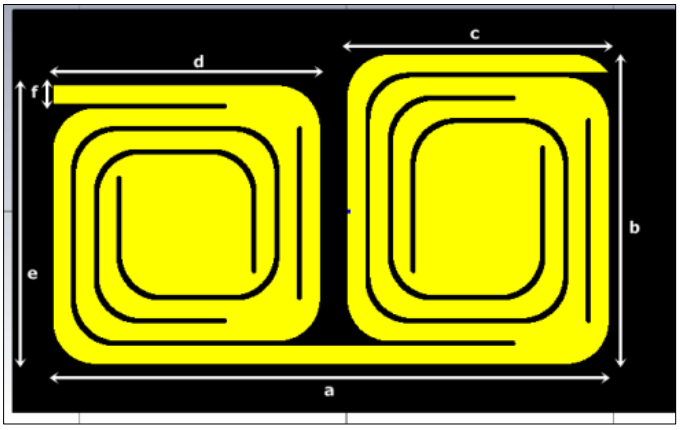

Figure 2a: The Antenna Design

Figure 2b: The Fabricated Antenna

Table II: The Dimension of Antenna Textile as the Result of Parametric Study [9]

NO	Parameter	Unit (mm)
1	Length of substrate	50
2	Width of substrate	30
3	Total Length of Patch (a)	41.6
4	Height of Substrate	3
5	Width of Line (f)	1.4
6	Width of Slot	0.3
7	Height of Patch	0.1
8	Length of Right Patch (c)	19.6
9	Width of Right Patch (b)	23.1
10	Length of Left Patch (d)	20
11	Width of Left Patch (e)	20.8
12	Distance of Spiral	2

The simulation was done by using software namely CST, while the direct measurement would be done according the scenario at the simulation and it would be done in an anechoic chamber. The scenario for simulation in this communication consisted of two types, i.e., *on-body* and *off-body* that the distances would be varied then.

For *on-body* LOS communication scenarios, the antenna textile would be placed upon the body part of visual nastran as shown in Figure 3a; this communication simulated the antenna as body worn antenna that is usually used for medical needs in human body.

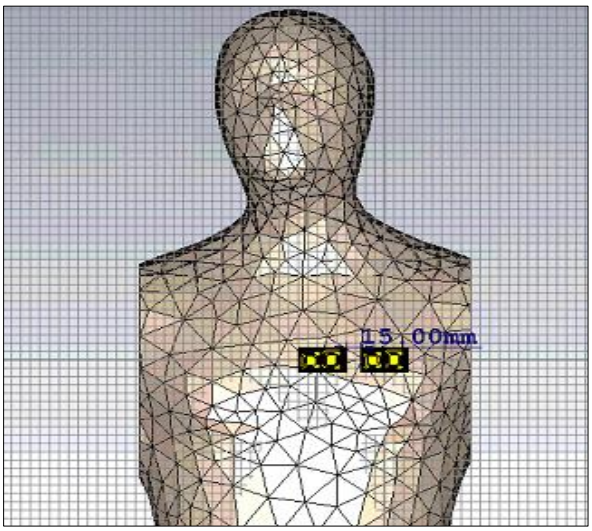

Figure 3a: On-Body LOS Scenario

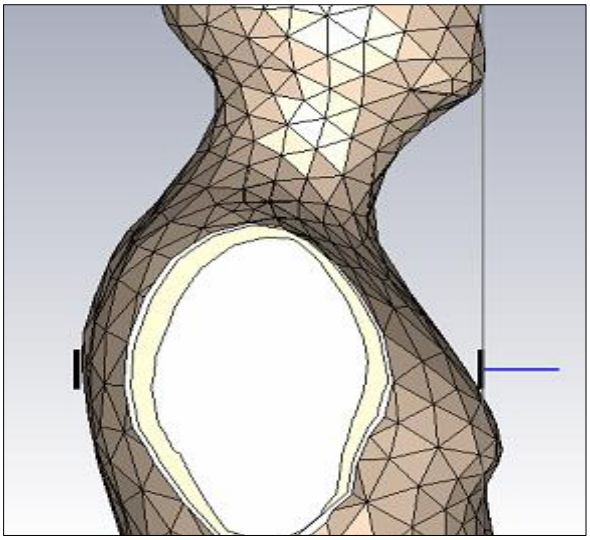

Figure 3b: On-Body NLOS Scenario

In this scenario, the variation of distance would be done four times for measurement i.e., 7.5 mm, 15 mm, 22.5 mm and 30 mm. Table III shows the simulation result that had been done for on-body scenario for LOS condition at frequency of RFID and ISM.

Table I: Simulation Result of *On-body* in LOS Condition

Distance (mm)	S_{21} (dB) RFID	S_{21} (dB) ISM
7.5	-42.129	-39.45
15	-49.056	-42.406
22.5	-51.102	-46.347
30	-54.03	-50.436

At *on-body for* NLOS condition, both antennas were placed on visual nastran model when it was blocked by *phantom* model as seen in Figure 3b. An antenna was placed on the chest and another was placed

around the back and then the variation distance was applied between the two of them. The data collection was done four times with distance variation per 100 mm. The result of data collection had been recorded in Table IV.

Table IV: The Result of *On-body* Simulation in NLOS Condition

Distance (mm)	S_{21} (dB) RFID	S_{21} (dB) ISM
400	-74.039	-80.164
500	-78.629	-85.036
600	-83.892	-90.841
700	-80.143	-87.958

At *off-body* in LOS condition, one of the antenna textiles was on the body part of visual nastran and another was not. Then, it was given a distance between both of them as in Figure 4a.

In this scenario, the variation distance was done four times for measurement i.e., 250 mm, 500 mm, 750 mm, and 1,000 mm. Table V shows the simulation result that had been done for each working frequency i.e., 924 MHz and 2.45 GHz.

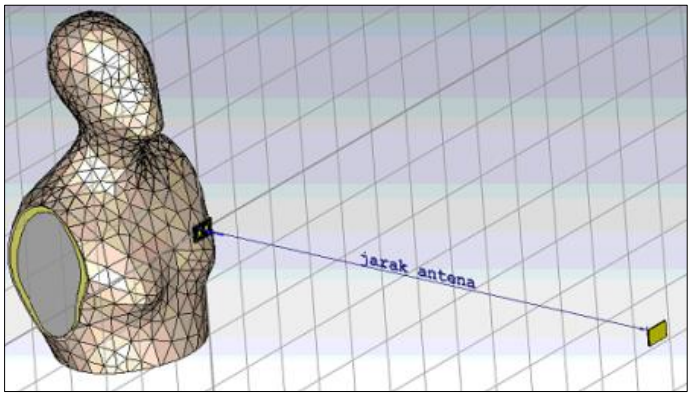

Figure 4a: Off-Body LOS Scenario

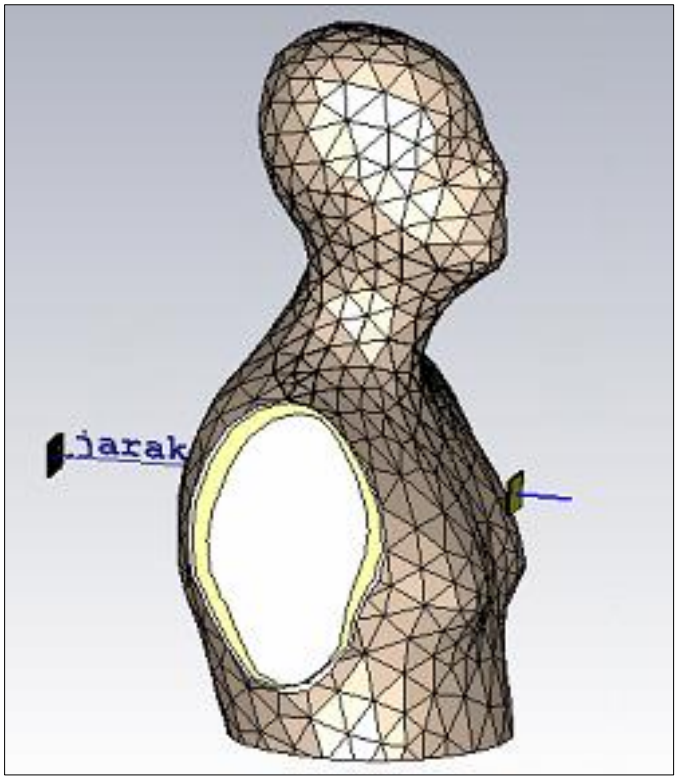

Figure 4b: On-Body NLOS Scenario

Table V: Simulation Result of *Off-body* in LOS Condition

Distance (mm)	S_{21} (dB) RFID	S_{21} (dB) ISM
250	-64.837	-49.515
500	-71.271	-55.921
750	-75.88	-59.236
1000	-78.013	-62.874

The *Off-body* scenario in NLOS condition as shown in Figure 4b, the antenna was placed at the front part of nastran model i.e., the chest. Yet, there was no antenna placed upon the other body, so there was a certain distance between the body and the antenna. It had been taken 4 data in this scenario for variation of each 5 cm. So, the result of data for each frequency i.e., 924 MHz and 2.45 GHz could be obtained as in Table VI.

Table VI: Simulation Result of *Off-body* in NLOS Condition

Distance (mm)	S_{21} (dB) RFID	S_{21} (dB) ISM
50	-93.058	-72.697
100	-95.079	-71.236
150	-98.201	-70.997
200	-117.06	-97.618

The data that had been collected from CST was the parameter value of $S_{21.}$ The absolute value of S_{21} showed the path loss value. The data that had been collected was then being processed and analyzed by a software namely MATLAB by using *fitted curve* method to obtain the estimation of propagation channels. The next step was calculating the *path loss exponent (n)* by using linear regression. Linear regression is method used for analyzing the correlation among variables. The correlation was expressed in form of equation that connected the dependent variable of *y* and independent variable of x that was written in equation 3. The variables in linear regression were connected to equation 1. *Y* value is *path loss* value taken from CST data in form of $|S_{21}|$. *a* is path loss value at reference distance ($P_{0,dB}$); in this calculation, the reference distance was 1 mm. *b* is the value from *10n* and *n* is path loss exponent value. Meanwhile, *x* is the value from $log_{10}(\frac{d}{d_0})$.

$$y = a + \text{bx} \qquad (3)$$

The calculation for measurement result was done by taking sample for ten times and then it would be averaged to find the value of standard deviation. The *path loss* value obtained by calculating the mean value would be processed using the similar steps for simulation process i.e., by using linear regression to find exponent path loss value, so the estimation of propagation channels could be found.

The measurement result of S_{21} at 924 MHz and 2.45 GHz for *on-body* communication in LOS condition obtained some values as shown in Table VII for variation distance.

Table VII: Measurement Result of *On-body* in LOS Condition

Distance	S_{21} (dB) RFID	σ Standard Deviation	S_{21} (dB) ISM	σ Standard Deviation
7.5	-28.1045	1.36	-33.4498	2.6
15	-32.1057	1.13	-34.6419	2.7
22.5	-40.7061	8.64	-46.7390	9.01
30	-38.0165	8.24	-42.0532	4.42

The measurement result of S_{21} at 924 MHz and 2.45 GHz for *on-body* communication in NLOS condition obtained some values as shown in Table VIII for variation distance.

Table VIII: Measurement Result of *On-body* in NLOS Condition

Distance	S_{21}(dB) RFID	σ	S_{21} (dB) ISM	σ
400	-64.4723	3.12	-70.1153	4.90
50	-68.4745	3.43	-72.7204	6.35
600	-70.944	3.31	-78.9164	8.93
700	-72.0968	3.74	-77.7275	3.98

The measurement result of S_{21} at 924 MHz and 2.45 GHz for *off-body* communication in LOS condition obtained some values as follows. The variation distance is shown in Table IX.

Table IX: Measurement Result of S_{21} for *Off-body* in LOS Condition

Distance (mm)	S_{21}(dB) RFID	σ	S_{21}(dB) ISM	σ
250	-32.0134	1.17	-38.8329	3.57
500	-37.8265	1.81	-43.4598	5.50
750	-40.4076	3.08	-47.7002	1.98
1000	-45.9880	1.81	-54.0247	2.02

The measurement result of S_{21} at 924 MHz and 2.45 GHz for *off-body* communication in NLOS condition obtained some values as seen in Table X for variation distance.

Table X: Measurement Result of S_{21} for *Off-body* in NLOS Condition

Distance (mm)	S_{21}(dB) RFID	σ	S_{21}(dB) ISM	σ
50	-67.3602	5.83	-69.0154	4.05
100	-74.5687	5.36	-78.8432	7.08
150	-78.8639	4.69	-85.0874	6.35
200	-86.0589	3.76	-92.5937	5.88

IV. RESULT OF SIMULATION, MEASUREMENT AND THE ANALYSIS

These are all scenarios from the two frequencies and the descriptions:

(1) = *on-body* scenario in LOS Condition.
(2) = *on-body* scenario in NLOS Condition.
(3) = *off-body* scenario in LOS Condition.
(4) = *off-body* scenario in NLOS Condition.

D. Scenario (1) for Simulation and Measurement at 924 MHz and 2.45 GHz.

The difference among path loss exponent values is not really significant. It can be seen from the recapitulation result in Table XI and the characteristic of graphic forms below.

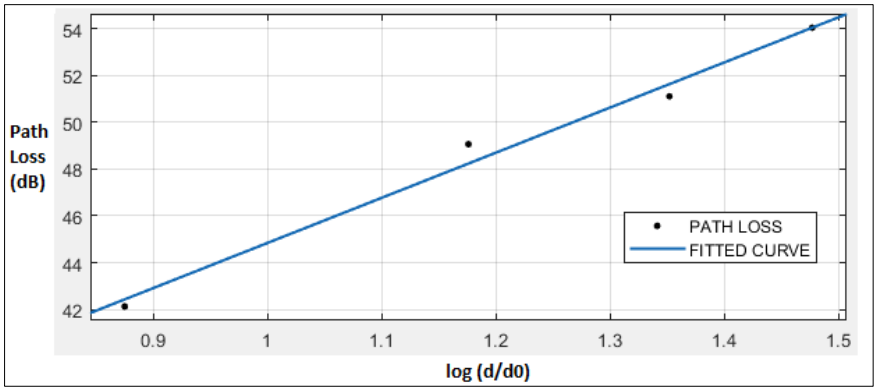

Figure 5: Simulation Result of Scenario 1 at 924 MHz

$$P_{dB}(d) = P_{0,dB} + 19.261\ log_{10}(\frac{d}{d_0}) \qquad (4)$$

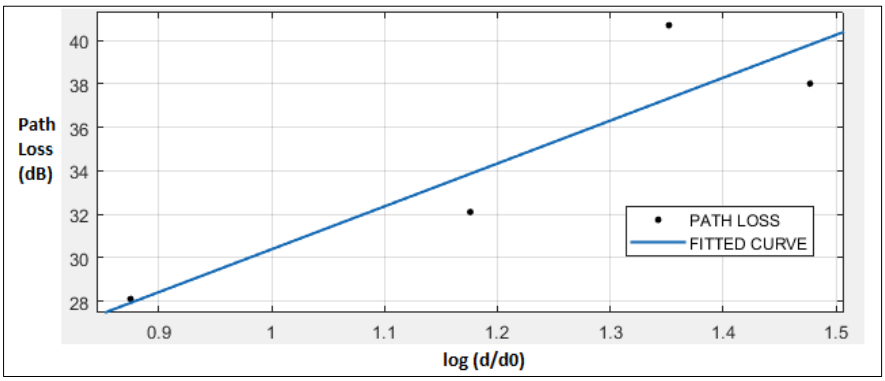

Figure 6: Measurement Result of Scenario 1 at 924 MHz

$$P_{dB}(d) = P_{0,dB} + 19.7361\ log_{10}(\frac{d}{d_0}) \qquad (5)$$

Meanwhile, the result of graphic for simulation and measurement at 2.45 GHz can be seen in Figure 7 and Figure 8.

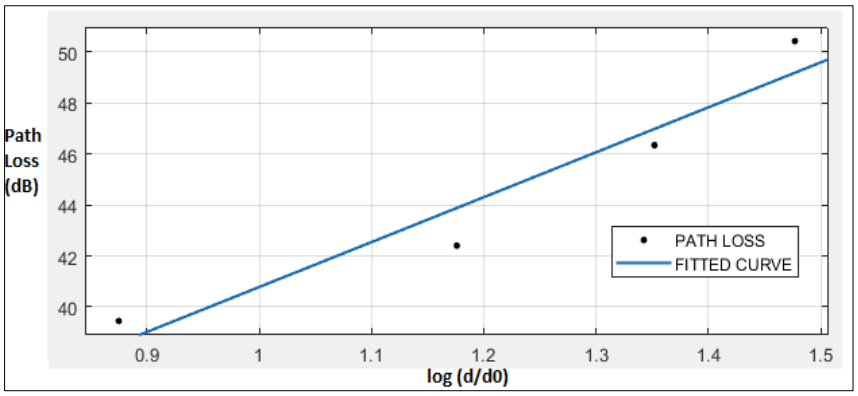

Figure 7: Simulation Result of Scenario 1 at 2.45 GHz

$$P_{dB}(d) = P_{0,dB} + 17.621\ log_{10}(\frac{d}{d_0}) \qquad (6)$$

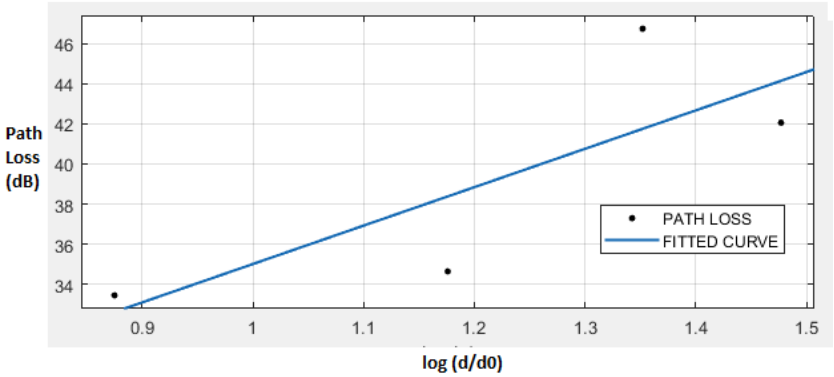

Figure 8: Measurement Result of Scenario 1 at 2.45 GHz

$$P_{dB}(d) = P_{0,dB} + 19.1361\ log_{10}(\frac{d}{d_0}) \qquad (7)$$

The path loss exponent value is greater than the simulation value. It is caused by the condition of test room for measurement that is less than ideal and the other objects that affect the propagation channels. Yet, there is no significant difference between path loss exponent values in measurement and path loss exponent values in simulation.

E. Scenario (2) for Simulation and Measurement at 924 MHz and 2.45 GHz.

The following is the graphic and the equation. Each graphic represents each frequency in scenario 2.

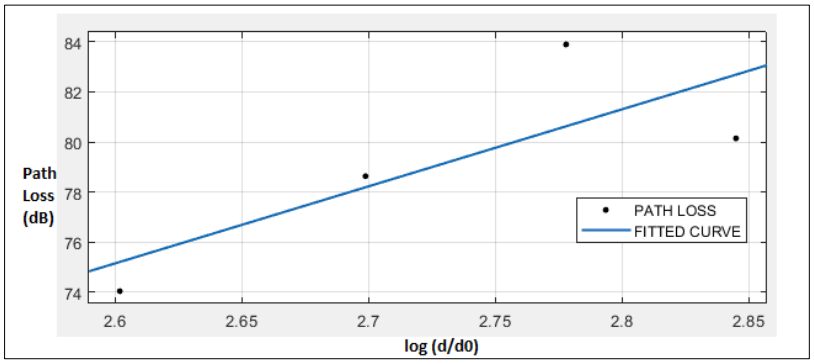

Figure 9: Simulation Result of Scenario 2 at 924 MHz

$$P_{dB}(d) = P_{0,dB} + 30.078\ log_{10}(\frac{d}{d_0}) \qquad (8)$$

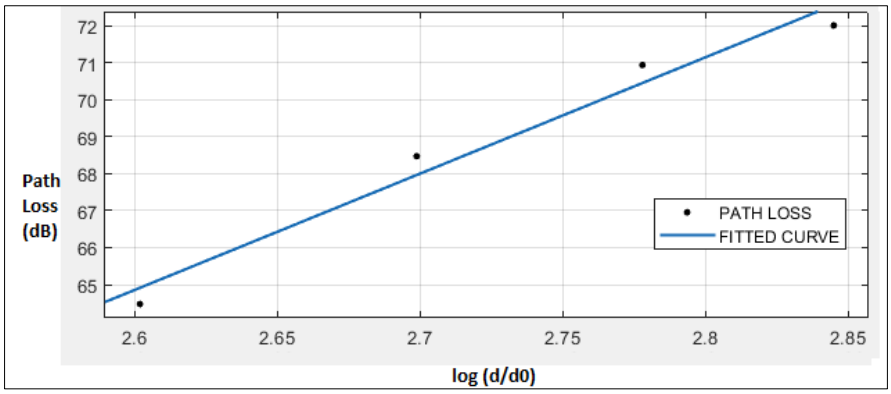

Figure 10: Measurement Result of Scenario 2 at 924 MHz

$$P_{dB}(d) = P_{0,dB} + 31.7963\ log_{10}(\frac{d}{d_0}) \quad (9)$$

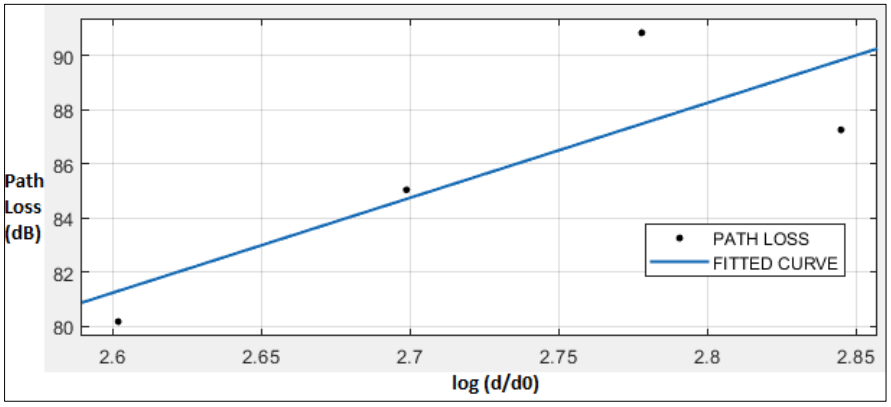

Figure 11: Simulation Result of Scenario 2 at 2.45 GHz

$$P_{dB}(d) = P_{0,dB} + 35.123\ log_{10}(\frac{d}{d_0}) \quad (10)$$

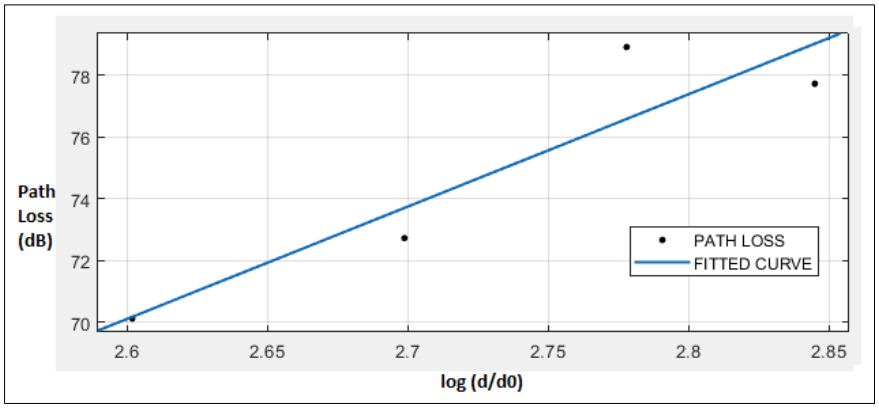

Figure 12: Measurement Result of Scenario 1 at 2.45 GHz

$$P_{dB}(d) = P_{0,dB} + 36.446\ log_{10}(\frac{d}{d_0}) \quad (11)$$

The result from the graphic and the equation is not really different from the result in scenario 1. It is caused by the similar problems that are occurred in the previous scenario. It shows that the gradient level for measurement is greater than simulation.

F. Scenario (3) for Simulation and Measurement at 924 MHz and 2.45 GHz.

These are the graphic and the equation. Each graphic represents each frequency in scenario 3.

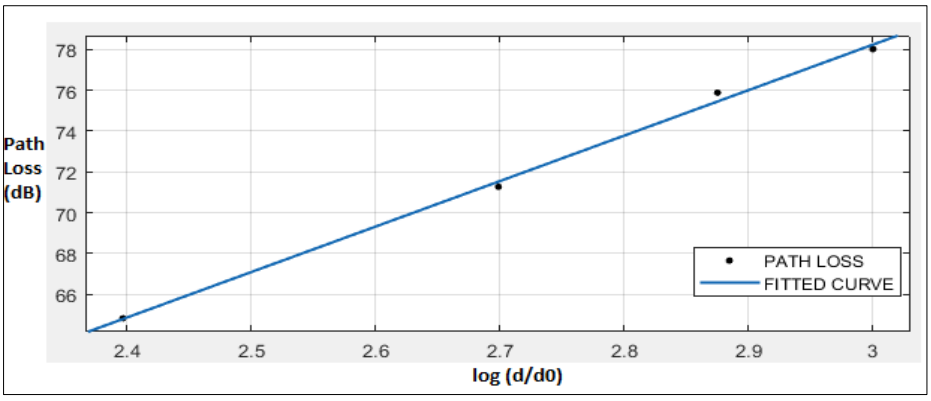

Figure 13: Simulation Result of Scenario 3 at 924 MHz

$$P_{dB}(d) = P_{0,dB} + 22.3063\ log_{10}(\frac{d}{d_0}) \qquad (12)$$

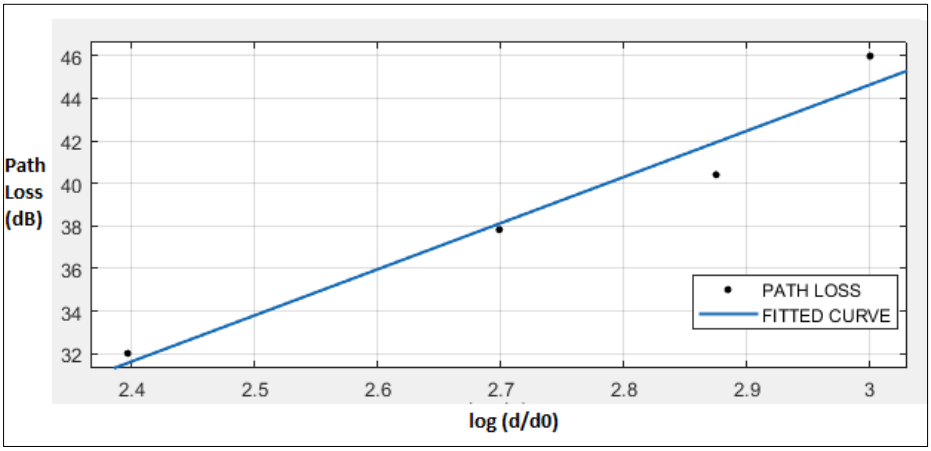

Figure 14: Measurement Result of Scenario 3 at 924 MHz

$$P_{dB}(d) = P_{0,dB} + 21.6976\ log_{10}(\frac{d}{d_0}) \qquad (13)$$

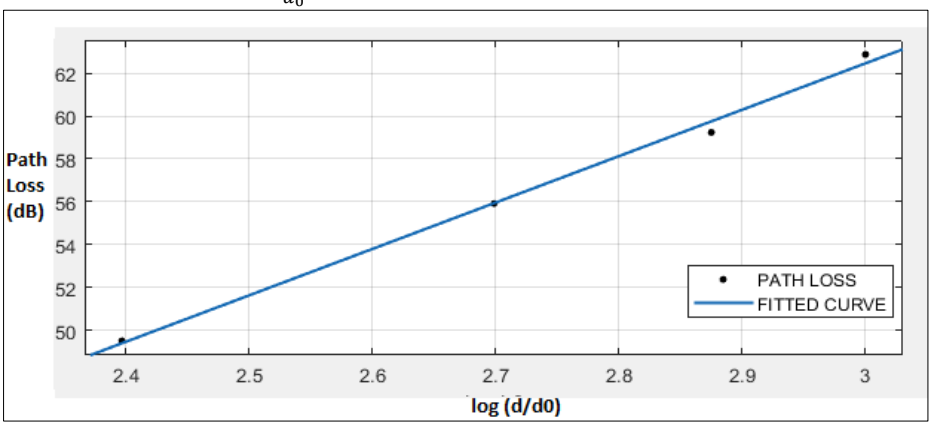

Figure 15: Simulation Result of Scenario 3 at 2.45 GHz

$$P_{dB}(d) = P_{0,dB} + 21.657\ log_{10}(\frac{d}{d_0}) \qquad (14)$$

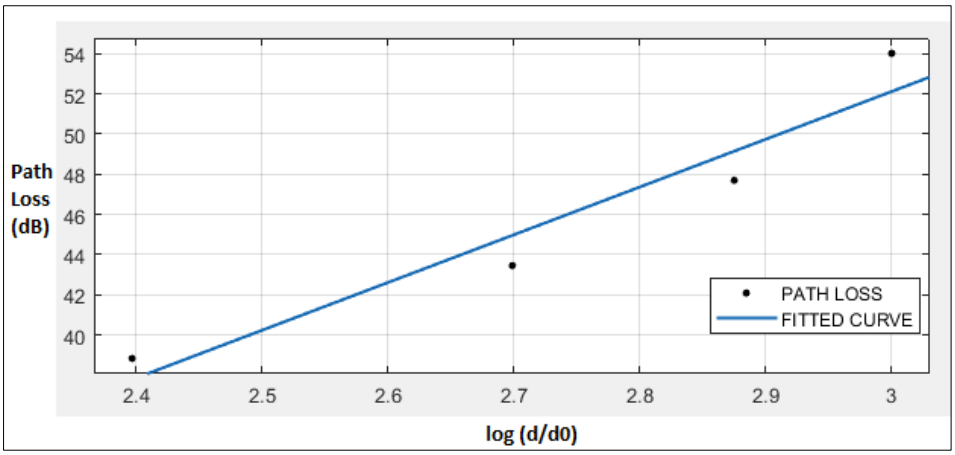

Figure 16: Simulation Result of Scenario 3 at 2.45 GHz

$$P_{dB}(d) = P_{0,dB} + 23.7827\ log_{10}(\frac{d}{d_0}) \quad (15)$$

In scenario 3 for 924 MHz, it has difference where the path loss exponent value is smaller than simulation. It caused by the position of antenna is less accurate when the measurement is being applied, and the difference in body size that is simulated and measured. Meanwhile, for 2.45 GHz, it has similar difference of characteristic as the previous scenarios have.

G. Scenario (4) for Simulation and Measurement at 924 MHz and 2.45 GHz.

These are the graphic and the equation. Each graphic represents each frequency in scenario 4.

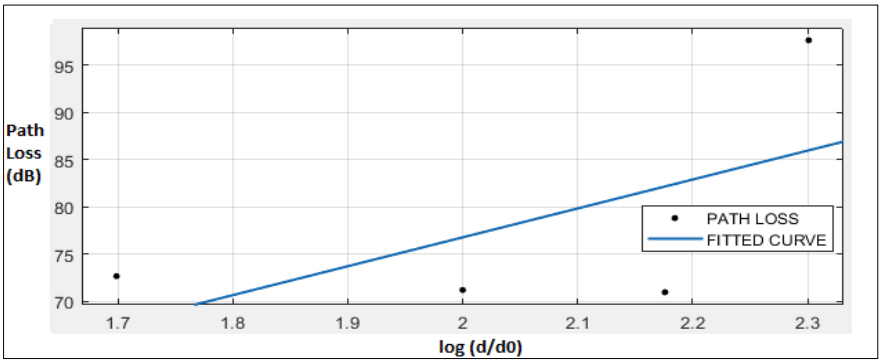

Figure 17: Simulation Result of Scenario 4 at 924 MHz

$$P_{dB}(d) = P_{0,dB} + 31.0592\ log_{10}(\frac{d}{d_0}) \quad (16)$$

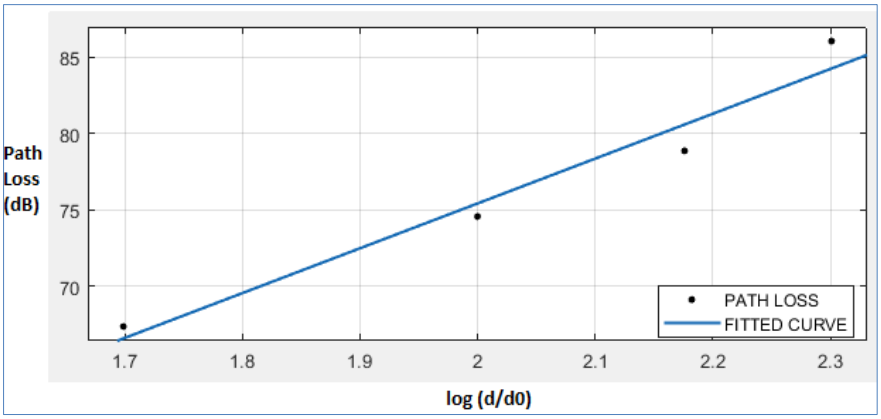

Figure 18: Measurement Result of Scenario 4 at 924 MHz

$$P_{dB}(d) = P_{0,dB} + 33.0521\ log_{10}(\frac{d}{d_0}) \quad (17)$$

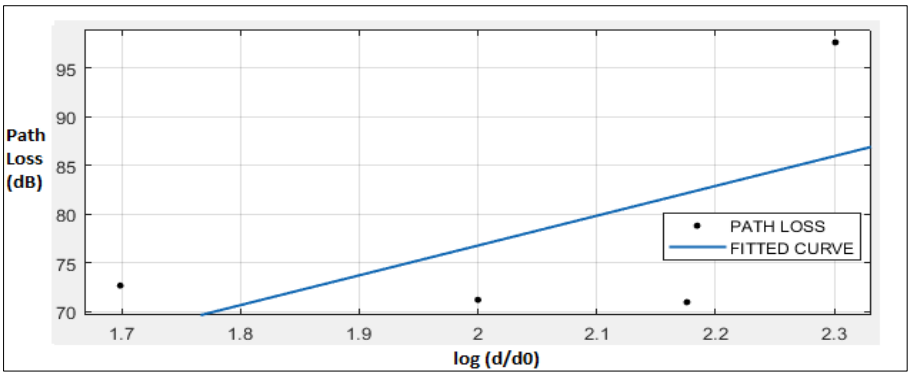

Figure 19: Simulation Result of Scenario 4 at 2.45 GHz

$$P_{dB}(d) = P_{0,dB} + 30.5373\ log_{10}(\frac{d}{d_0}) \quad (18)$$

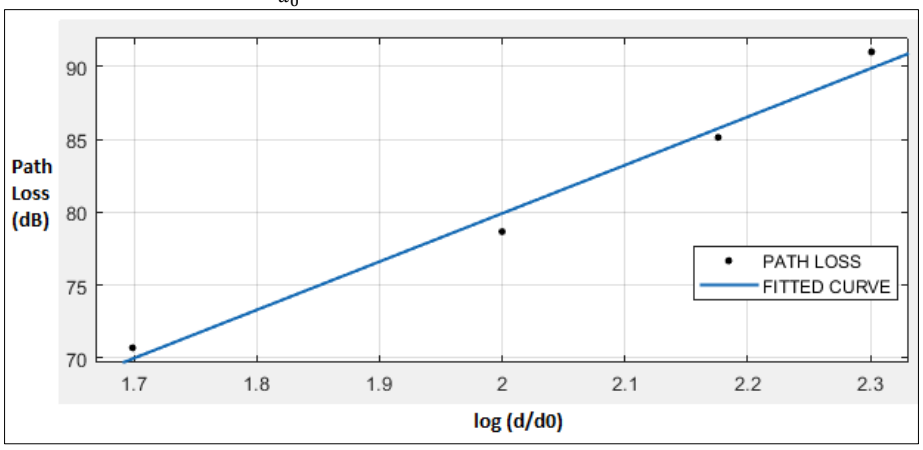

Figure 20: Measurement Result of Scenario 4 at 2.45 GHz

$$P_{dB}(d) = P_{0,dB} + 33.15\ log_{10}(\frac{d}{d_0}) \quad (19)$$

In scenario 4, the difference of path loss exponent value is quite far. It can be seen from the gradient of graphic. This can be affected by various factors. One of the main factors is the difference in body size for simulation and measurement, the condition of test room when conducting simulation and measurement and also other surrounding distortions when measurement is in progress. Another factor that causes this happened is the position of antenna on the body between the simulation and measurement that is less accuracy. So, it affects the path loss value that had been obtained from one to another. For the simulation itself, it does not model the whole human body, but the upper part of the body only. It, of course, affects the characteristic of propagation, so the value between simulation and measurement is quite different.

Table XI: Recapitulation of Path Loss Exponent Calculation Result

Frequencies	Scenarios	n Simulation	n Measurement
RFID (924 MHz)	1	1.9261	1.97361
	2	3.07857	3.17963
	3	2.23063	2.16976
	4	3.30521	2.93776
ISM (2.45 GHz)	1	1.76251	1.91397
	2	3.5123	3.64486
	3	2.16547	2.37827
	4	3.05373	3.315

V. IMPLEMENTATION

The implementation is done by using arduino and nrf2401 as the devices to obtain the result of heart rate interpretation from the subject. The tool works at 2.4-2.5 GHz, so the data is collected only by based on one of working frequency of antenna i.e., 2.45 GHz.

Table XII: Recapitulation of Path Loss Exponent Calculation Result

Subject	Age (Years Old)	Weight (Kg)	Gender
1	6	24	Female
2	25	79	Male
3	56	63	Female

Figure 21: The Antenna Position in Subject 1-3 from left to right

The position of transmitting antenna is shown in Figure 21 for each subject i.e., at the left arm of the subject. Meanwhile, the receiving antenna is placed as shown in Figure 22, so the scenario for this experiment is *off-body* communication in NLOS condition that is blocked by wall.

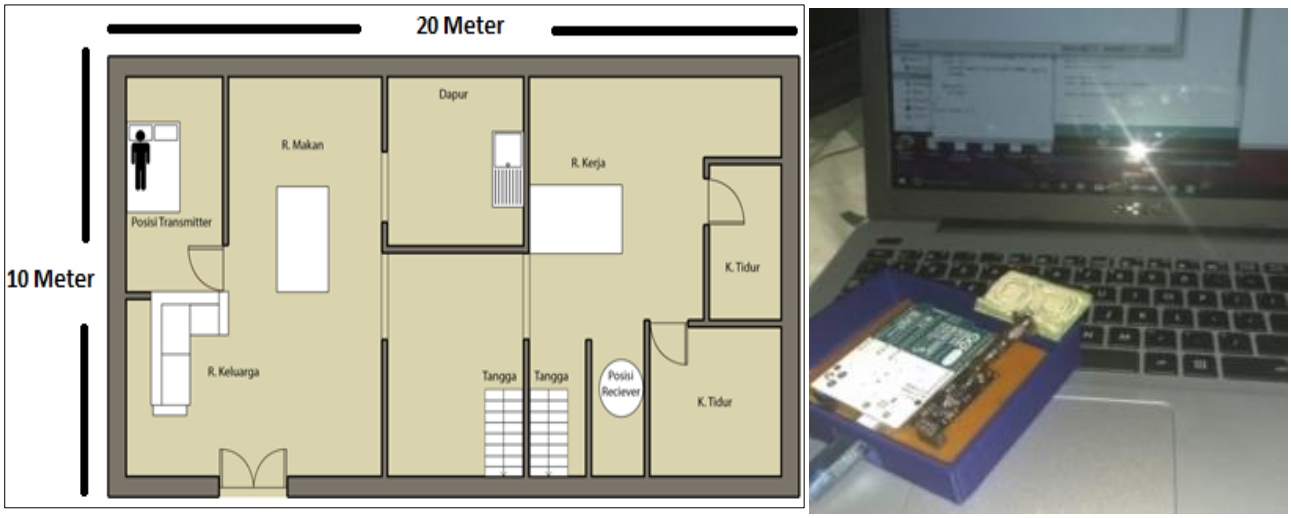

Figure 22: Map for the Antenna Positions

The result of ECG interpretation for subject 1, 2, and 3 in the *off-body* NLOS scenario, in order, is presented in Figure 23a, Figure 23b, and Figure 23c.

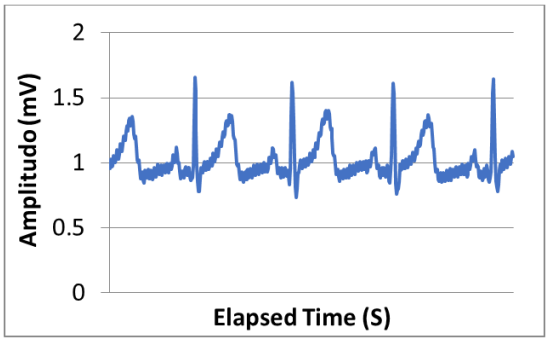

Figure 23a: Result of ECG Interpretation in Subject 1

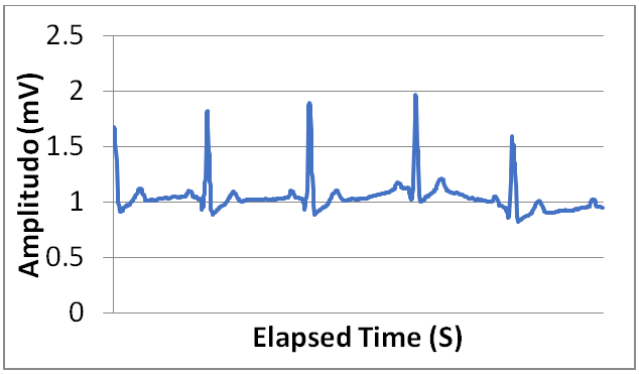

Figure 23b: Result of ECG Interpretation in Subject 2

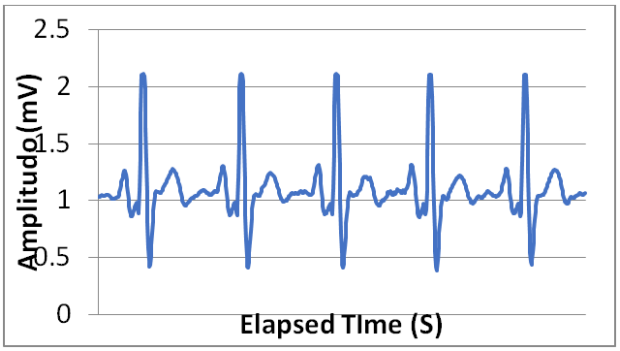

Figure 23c: Result of ECG Interpretation in Subject 3

Based on the result of observation towards heart rate in the graphic above, the difference can be seen for the age variation. So, it can be concluded that the age differences and gender affect the characteristic from each heart rate. Then, for subject 1, there is *ripple* in the interpretation result since the age from the subject is quite young. So, it cannot be relax when it is monitored and it caused little trouble on the tool. Yet, the overall characteristic from the heart rate can still be seen. Besides, the result from the implementation above also shows that each range of age has different characteristic of heart rate. In the graphic, it also shows that the characteristic of woman's heart has higher T wave amplitude than the man's heart has. It is also happened for QRS wave.

In a whole, this shows that antenna textile from *on-body* and *off-body* communication in NLOS condition can work well in the implementation of data sending.

VI. CONCLUSION

Simulation and measurement of *on-body* and *off-body* communication propagation channels by using dual-band magnetic antenna textile has been done.

Simulation and measurement of *on-body* and *off-body* communication has been done and it shows different characteristic according to the environment shown in n value (*path loss* exponent). In addition, the result in the simulation and measurement shows that human body has significant impact towards *path loss* exponent value and it has special characteristic. The difference of *path loss* value between simulation and measurement happened because of some factors, especially from the material of antenna between simulation and fabrication, the position of body and the condition of test room for measurement.

The fabricated antenna using thread that is embroidered and then layered by conductive paint can work well and it is implemented successfully at data sending system of ECG.

REFERENCES

1. World Health Organization. (2017). WHO Library Cataloguing-in-Publication Data Telemedicine: opportunities and developments in Member States: report on the second global survey on eHealth 2010. *Global Observatory for eHealth Series, 2*. Available from: http://www.who.int/goe/publications/goe_telemedicine_2010.pdf.
2. Zimmerman, T. G. (1995). Personal Area Networks (PAN): Near-Field IntraBody Communication, in Media Art and Science, *Master Thesis: Massachusetts Institute of Technology*.
3. Srinivasa, S., dan Haenggi, M. Path Loss Exponent Estimation in Large Wireless Networks. *University of Notre Dame, USA.*
4. Cotton, S. L., McKernan, A., Ali, A. J., & Scanlon, W. G. (2011). *An Experimental Study on the Impact of Human Body Shadowing in Off-Body Communications Channels at 2.45 GHz*. UK: EuCAP.

5. Jalil, M. E. B., Abd Rahim, M. K., Samsuri, N. A., Murad, N. A., Majid, H. A., Kamardin, K., & Abdullah, M. A. (2013). Fractal koch multiband textile antenna performance with bending, wet conditions and on the human body. *Progress In Electromagnetics Research*, *140*, 633-652.
6. Hall, P. S., dan Hao, Y. (2006). Antennas and Propagation for Body-CentricWireless Communications. *Artech House.*
7. Reusens, E., Joseph, W., Vermeeren, G., Kurup, D., & Martens, L. (2008, June). Real human body measurements, model, and simulations of a 2.45 GHz wireless body area network communication channel. In *2008 5th International Summer School and Symposium on Medical Devices and Biosensors* (pp. 149-152). IEEE.
8. Anthony, O. N., & Okonkwo Obikwelu, R. (2014). Characterization of signal attenuation using pathloss exponent in South-South Nigeria. *International Journal of Emerging Trends & Technology in Computer Science (IJETTCS)*, *3*(3).
9. Basari, A., Wahid, F. Y., Zulkifli, E. T., & Rahardjo. (2016). Dual-Band Magnetic Antenna Textile for Body Area Network Application. *Universitas Indonesia*.